

Inhibition of the spindle assembly checkpoint kinase TTK enhances the efficacy of docetaxel in a triple-negative breast cancer model

A. R. R. Maia¹, J. de Man², U. Boon³, A. Janssen^{1,†}, J.-Y. Song⁴, M. Omerzu⁵, J. G. Sterrenburg², M. B. W. Prinsen², N. Willemsen-Seegers², J. A. D. M. de Roos², A. M. van Doornmalen², J. C. M. Uitdehaag², G. J. P. L. Kops^{5,6}, J. Jonkers^{3,6}, R. C. Buijsman², G. J. R. Zaman^{2*} & R. H. Medema^{1,6}

¹Division of Cell Biology, The Netherlands Cancer Institute, Amsterdam; ²Netherlands Translational Research Center B.V., Oss; Divisions of ³Molecular Pathology and Cancer Genomics Centre; ⁴Experimental Animal Pathology, The Netherlands Cancer Institute, Amsterdam; Departments of ⁵Medical Oncology; ⁶Cancer Genomics Netherlands, UMC Utrecht, Utrecht, The Netherlands

Received 26 June 2015; accepted 29 June 2015

Background: Triple-negative breast cancers (TNBC) are considered the most aggressive type of breast cancer, for which no targeted therapy exists at the moment. These tumors are characterized by having a high degree of chromosome instability and often overexpress the spindle assembly checkpoint kinase TTK. To explore the potential of TTK inhibition as a targeted therapy in TNBC, we developed a highly potent and selective small molecule inhibitor of TTK, NTRC 0066-0.

Results and Conclusions: The compound is characterized by long residence time on the target and inhibits the proliferation of a wide variety of human cancer cell lines with potency in the same range as marketed cytotoxic agents. In cell lines and in mice, NTRC 0066-0 inhibits the phosphorylation of a TTK substrate and induces chromosome missegregation. NTRC 0066-0 inhibits tumor growth in MDA-MB-231 xenografts as a single agent after oral application. To address the effect of the inhibitor in breast cancer, we used a well-defined mouse model that spontaneously develops breast tumors that share key morphologic and molecular features with human TNBC. Our studies show that combination of NTRC 0066-0 with a therapeutic dose of docetaxel resulted in doubling of mouse survival and extended tumor remission, without toxicity. Furthermore, we observed that treatment efficacy is only achieved upon co-administration of the two compounds, which suggests a synergistic *in vivo* effect. Therefore, we propose TTK inhibition as a novel therapeutic target for neoadjuvant therapy in TNBC.

Key words: TTK/Mps1 kinase inhibitor, docetaxel, chromosome missegregation, triple-negative breast cancer, increased survival

introduction

Breast cancer is a complex disease conventionally subtyped according to gene expression profile. Among these subtypes, triple-negative breast cancer (TNBC) is characterized by the absence of estrogen receptor (ER), progesterone receptor and human epidermal growth factor receptor type 2 (HER) [1]. These tumors are typically high grade, associated with cellular pleomorphism and a high mitotic index, a hallmark of chromosomal instability (CIN).

Due to the lack of hormone receptors and HER2 expression, patients do not respond to hormone therapy or tyrosine kinase inhibitors, placing TNBC patients in a high-risk group [2]. TNBC patients are often treated with taxanes, but despite good response to therapy, their survival rates are not profoundly changed [3]. Thus, there is a need for novel and more efficacious treatments of TNBC.

In the past decade, genomic and proteomic profiling of human breast cancer samples has improved the understanding and the molecular characterization of TNBC. In particular, high levels of TTK mRNA and protein were found in samples from patients with TNBC [4–6]. The protein kinase TTK (commonly referred to as Mps1) is a component of the Spindle Assembly Checkpoint (SAC) [7], a surveillance mechanism that ensures the fidelity of chromosome segregation. Defects in SAC functioning can lead to

*Correspondence to: Dr Guido Zaman, Netherlands Translational Research Center B.V., Molenstraat 110, 5340 AG Oss, The Netherlands. Tel: +31-412-700500; E-mail: guido.zaman@ntrc.nl

[†]Present address: Division of Life Sciences, Lawrence Berkeley National Lab, University of California at Berkeley, Berkeley, CA 94720, USA.

chromosome segregation errors by allowing mitotic exit in the presence of unattached kinetochores [8]. Complete loss of SAC function is lethal in mice [9] and incompatible with viability of human cell lines [10, 11]. In addition to breast cancer, TTK mRNA levels are elevated in other human cancers, including thyroid papillary carcinoma, hepatocellular carcinoma, pancreatic ductal adenocarcinoma, glioma, gastric, bronchogenic and lung [5, 6, 12–19]. In most cases, high levels of TTK expression correlate with an increase in copy number of the TTK gene [6].

Earlier studies propose that high levels of TTK might be needed to sustain an abnormal number of chromosomes [5], a state that is called ‘aneuploid’. Aneuploidy is a common feature of solid human tumors [20] and a predictor of poor prognosis in breast, lung, brain and colorectal cancer [18, 21–23]. High levels of TTK could prevent aneuploid tumor cells to undergo massive chromosome gains or losses during mitosis that could subsequently compromise their viability. Indeed, TTK is one of the genes included in the molecular signature of chromosome instability in human cancer—CIN70 [21]. This suggests that TTK inhibitors could specifically hamper cells that express high levels of TTK, and as a consequence, increase CIN and reduce cell viability. These observations have led to a search for specific TTK kinase inhibitors for the treatment of cancer. A number of these inhibitors have been shown to reduce growth of xenografts of melanoma [24], colorectal carcinoma [25–27], cervical carcinoma [25] and glioblastoma [18] cells in mice. However, the effect of treatment with TTK inhibitors in mouse models that mimic TNBC has not been determined, despite the correlative evidence that TTK may be a good therapeutic drug target for TNBC [4, 6].

The standard of care treatment in TNBC patients is neoadjuvant chemotherapy followed by radiotherapy and surgery [2]. Treatment with taxane drugs (such as docetaxel or paclitaxel) is common in this group of patients. However, safety issues limit the clinical application of taxanes, namely, acute bone marrow toxicity and cumulative peripheral sensible neurotoxicity [28, 29]. Targeted agents that allow taxanes to be administered at a lower dose while maintaining the same efficacy could provide a significant benefit in the treatment of TNBC patients.

Here, we describe a novel small molecule inhibitor of TTK, NTRC 0066-0, which inhibits TTK enzyme activity with subnanomolar IC_{50} , and shows very potent antiproliferative activity on a broad panel of human cancer cell lines. Most importantly, the combination of NTRC 0066-0 and docetaxel increases the survival in a murine breast cancer model that mimics human TNBC and delays tumor relapse, suggesting that this might be a clinically valuable combination.

materials and methods

kinase inhibitors

NTRC 0066-0 was designed and synthesized at Netherlands Translational Research Center B.V. (NTRC) as described in the Supplemental Experimental Procedures (supplementary Material, available at *Annals of Oncology* online). Reference TTK inhibitors Mps-Bay-2b and MPI-0479605 were synthesized at NTRC according to published protocols [25, 27]. Structure of the compounds was confirmed by mass spectroscopy and nuclear magnetic resonance. Most other kinase reference inhibitors and cytostatic agents were purchased from commercial vendors (supplementary Table S8, available at *Annals of Oncology* online).

kinase assays

The inhibitory activity of compounds on biochemically purified full-length TTK was determined in the IMAP[®] assay (Molecular Devices, Sunnyvale, CA) as described in the Supplemental Experimental Procedures (supplementary Material, available at *Annals of Oncology* online). Activity of TTK inhibitors on full-length Aurora A, Aurora C, PLK1 and PLK4 (Carna Biosciences, Inc., Kobe, Japan) was determined in LANCE[®] Ultra TR-FRET assays (Perkin Elmer, Groningen, The Netherlands). Broad kinase selectivity profiling was carried out at Carna.

cell proliferation assays

All cell lines were purchased from the American Type Culture Collection (ATCC, Manassas, VA) and cultured as recommended by ATCC. All cells used were within nine passages of the original ATCC vial. Proliferation assays were carried out in 384-well plates with incubation with compound for either 72 h (3 days) or 120 h (5 days) as described [30]. To determine the effect of NTRC 0066-0 on colony formation, HCT-116 or PA-1 cells were seeded at a density of 3200 cells per well in 6-well plates. After 4 h incubation in a humidified atmosphere of 5% CO_2 at 37°C, a dilution series of compound was added, and incubation was continued. After 5 days, cells were fixed with Leishman’s Eosin. Plates were scanned with a flatbed scanner and number of colonies determined with Image J software.

live cell imaging

HeLa cells stably expressing H2B-YFP were plated in 6-well glass bottom plates (LabTek Corp., Australia) and treated with NTRC 0066-0 or vehicle. Cells were imaged every 5 min in Leibovitz L15 CO_2 -independent cell culture medium in a heated chamber at 37°C, using a $\times 40$ NA 0.95 air objective on an IX71 microscope (Olympus) controlled by SoftWoRx 6.0 software (Applied Precision). Image Z-stacks were acquired with 2- μm intervals using an sCMOS camera (DeltaVision RT; Applied Precision, GE Healthcare, Issaquah, WA) and processed using ImageJ and Adobe Photoshop.

intervention studies

Tumors were generated in *K14cre;Brca1^{fl/fl};TP53^{fl/fl}* female mice and samples were cryopreserved. Orthotopic transplantation of *BRCA1^{-/-};TP53^{-/-}* tumors in wild-type FVB mice was carried out as previously described [31]. The tumor size was monitored at least three times a week by caliper measurements. The tumor volume was calculated with the formula: $0.5 \times \text{length} \times \text{width}^2$. Animals were euthanized by CO_2 asphyxiation in case of signs of drug toxicity or if tumors reached a maximum size of 1500 mm^3 . The Animal Ethics Committee of the Netherlands Cancer Institute approved all animal experiments. The MDA-MB-231 xenograft study was carried out at Oncodesign (Dijon, France).

histopathology

Formalin-fixed paraffin-embedded (FFPE) tumors were sectioned at 4 μm and stained with hematoxylin and eosin for histological evaluation according to standard procedures. For immunohistochemistry, sections were stained with antibody against TTK MELP1^{943/1155} [32]. For immunofluorescence, sections were stained using citrate antigen retrieval protocol with phospho-Histone H3 (Ser10) (06-570, Millipore), and Alexa 568 anti-rabbit (A-11011, Life technologies). DNA was counterstained with DAPI.

statistical analysis

Kaplan–Meier survival curves were analyzed by log-rank test (GraphPad Prism v6.0f), with a level of significance of $P < 0.05$. Overall survival was calculated as time from first treatment to death from any cause. Statistical

analysis of chromosome segregation in cell lines was carried out with GraphPad Prism v6.0f as indicated in the figures.

data and materials availability

NTRC 0066-0 can be obtained for research purposes through an MTA from Netherlands Translational Research Center B.V. (submit request to GJRZ).

results

biochemical characterization of a novel selective TTK inhibitor

We have developed a novel small molecule inhibitor of TTK, NTRC 0066-0 (Figure 1A), with potent activity in cell proliferation assays (Table 1), and used this compound to investigate the potential application of TTK inhibition as a novel therapeutic strategy for TNBC. NTRC 0066-0 inhibits TTK enzyme activity with IC_{50} of 0.6 nM and was more than 200 times selective over 276 kinases examined, including the mitotic kinases Aurora C, PLK1, PLK4 (Figure 1B, Table 1, supplementary Table S1, available at *Annals of Oncology* online).

The biochemical and cellular activity of NTRC 0066-0 was compared with that of three published reference inhibitors (Figure 1C). AZD-3146 is a research tool compound [33]. MPI-0497605 and Mps-Bay-2b are preclinical compounds from drug discovery programs of Myrex, Inc., and Bayer Pharma A.G., respectively [25, 27]. Our data confirmed the activity of the

reference inhibitors for TTK, as well as the inhibition of cancer cell line proliferation (Table 1). However, NTRC 0066-0 is 10–40 times more potent in cell proliferation assays (Table 1).

The binding kinetics of NTRC 0066-0 were determined by surface plasmon resonance using an immobilized TTK kinase domain (Figure 1C). Binding of NTRC 0066-0 to TTK was reversible, although the compound showed very slow dissociation kinetics, indicating a long target residence time (Figure 1C). Based on the association and dissociation constants, a binding affinity (K_D) was determined of 0.4 nM (Table 1), consistent with the IC_{50} of 0.6 nM in the enzyme activity assay of TTK (Figure 1B; Table 1). The other TTK reference inhibitors showed intermediate (MPI-0479605) or fast (Mps-Bay-2b, AZD-3146) dissociation kinetics (Figure 1C), consistent with their lower potency in the enzyme activity and cell proliferation assays (Table 1).

cancer cell line profiling

To characterize the cellular activity of NTRC 0066-0, we treated a broad range of cancer cell lines derived from different tumor tissues (Figure 2; supplementary Table S2, available at *Annals of Oncology* online) [30]. In proliferation assays with incubation time of 3 days, IC_{50} ranged from 18 to 897 nM, with an average IC_{50} of 67 nM (Figure 2A; supplementary Table S2, available at *Annals of Oncology* online). Most notably, there were strong differences in the maximum effect between the different cell lines (Figure 2B). For instance, NTRC 0066-0 almost completely

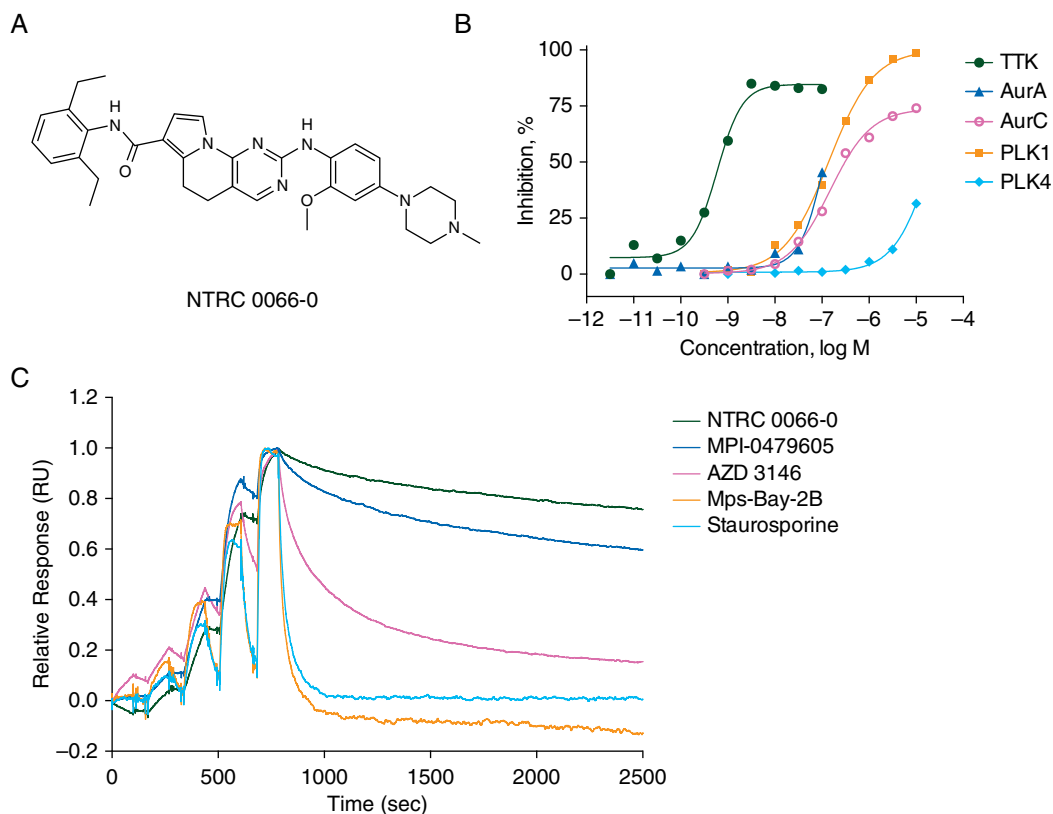


Figure 1. NTRC 0066-0 is a specific small molecule inhibitor for TTK. (A) Chemical structure of NTRC 0066-0. (B) Dose–response curves of NTRC 0066-0 in enzyme activity assays for TTK, Aurora A, Aurora C, PLK1 and PLK4. IC_{50} are, respectively, 0.6, 125, 162, 155 and >10 μ M. (C) Binding kinetics of NTRC 0066-0, TTK reference inhibitors and staurosporine determined by surface plasmon resonance. An overlay of representative graphs of single-cycle kinetics experiments is shown.

Table 1. Biochemical characterization and comparison of NTRC 0066-0 and reference TTK inhibitors in enzyme activity assays for TTK, Aurora A, Aurora C and PLK1, a surface plasmon resonance binding assay for TTK and cell proliferation assay with MOLT-4 cells

Compound	IC ₅₀ (M)	k _a (1/Ms)	TTK			t _{1/2} (s)	Aurora A	Aurora C	PLK1	Cell
			k _d (1/s)	K _D (M)	IC ₅₀ (M)		IC ₅₀ (M)	IC ₅₀ (M)	IC ₅₀ (M)	
NTRC 0066-0	0.6E-09	5.1E+05	2.2E-04	4.3E-10	3185	1.3E-07	1.6E-07	1.6E-07	2.6E-08	
AZD 3146	2.5E-09	3.5E+07	1.8E-01	5.0E-09	4	>1.0E-05	>1.0E-05	1.5E-06	1.2E-06	
MPI-0479605	2.6E-09	1.6E+06	9.7E-04	5.9E-10	718	3.2E-07	4.2E-06	>1.0E-05	3.2E-07	
Mps-Bay-2b	4.1E-09	2.2E+06	2.2E-02	1.0E-08	31	>1.0E-05	>1.0E-05	>1.0E-05	1.1E-06	
Staurosporine		6.7E+05	1.6E-02	2.5E-08	42					

IC₅₀ in enzyme activity were determined with full-length enzymes at K_{m, ATP}. Association constant (k_a), dissociation constant (k_d), binding constant (K_D) and half-life of enzyme-inhibitor complex (t_{1/2}) were determined by surface plasmon resonance using TTK kinase domain and Biacore T200. Values are means of two independent experiments.

inhibited the proliferation of MOLT-4 and PA-1 cells, whereas inhibition of HCT-116 and MDA-MB-231 was only partial after 3 days (Figure 2B). When cells were treated for 5 days, efficacy increased for most cell lines, including HCT-116 and MDA-MB-231 (Figure 2B; supplementary Table S2, available at *Annals of Oncology* online). This finding supports the idea that more cell divisions increase the likelihood of TTK inhibitor-induced mitotic errors [34]. The potent antiproliferative activity of NTRC 0066-0 was confirmed in colony formation assays with HCT-116 and PA-1 cells (Figure 2C).

The cancer cell line profile of NTRC 0066-0 was compared with that of other kinase inhibitors and reference compounds (Figure 2D). Like NTRC 0066-0, MPI-049605 inhibited the proliferation of all cell lines, although the compound was less potent than NTRC 0066-0 (Figure 2D; supplementary Table S2, available at *Annals of Oncology* online).

The broad antiproliferative activity of NTRC 0066-0 discriminates TTK inhibitors from other targeted kinase inhibitors, such as the EGFR inhibitor gefitinib and the Abl1 inhibitor imatinib, which selectively inhibit the proliferation of only a few cell lines in the panel [30]. TTK inhibitors have a similarly broad profile as other cell cycle kinase inhibitors, such as Aurora kinase, PLK1 and CDK inhibitors. Therefore, we compared the profile of NTRC 0066-0 with a representative set of these and other reference compounds (Figure 2D; supplementary Table S3, available at *Annals of Oncology* online). The most potent antiproliferative compound was docetaxel, with an average IC₅₀ across the cell panel of 4 nM (supplementary Table S3, available at *Annals of Oncology* online). With its average IC₅₀ of 67 nM, NTRC 0066-0 is equally potent as the PLK1 inhibitor volasertib (BI-6727) (65 nM), and doxorubicin (71 nM), and more potent than the Aurora, CDK, CHK1 and Wee1 inhibitors tested (supplementary Table S3, available at *Annals of Oncology* online).

After median scaling and clustering (Figure 2D), the TTK, PLK1, CHK1 and most CDK1 inhibitors all form separate clusters. Also the pan-Aurora and Aurora A inhibitors, and the classic cytotoxic therapies, such as docetaxel and vincristine, form separate clusters (Figure 2D). This indicates that SAC inhibition leads to different biological responses than inhibiting other cell cycle processes, even within spindle assembly. Notably, TTK inhibitors are relatively good at inhibiting the colon carcinoma cell line HCT-15 and the lung cancer cell line SHP-77, which is relatively resistant to drugs that perturb

microtubule dynamics (Figure 2D). Interestingly, there seems to be a mutual exclusivity between cell lines that respond well to docetaxel or vincristine, and cell lines that respond to NTRC 0066-0 or MPI-0479605: almost all cell lines that are relatively resistant to these microtubule drugs are particularly sensitive to TTK inhibition (Figure 2D). Also cell lines that are relatively resistant to Aurora kinase inhibitors are sensitive to TTK inhibition (Figure 2D, upper right). The different sensitivity patterns can in part be explained by the multidrug resistance mechanisms, such as present in the SHP-77 cell line [35]. Alternatively, differences in mechanism of action, i.e. spindle poisons activate the SAC [36], whereas NTRC 0066-0 inhibits it, might underlie the different cellular response profiles.

target engagement and mechanism of action studies

Having demonstrated that NTRC 0066-0 selectively inhibits TTK *in vitro*, we wanted to confirm target engagement in human cells. KNL1/CASC5 is a kinetochore scaffold protein that is phosphorylated by TTK at specific repeat sequences—MELT repeats [37]. The phosphorylation status of KNL1 was determined by immunostaining of mitotic HeLa cells in the presence or absence of NTRC 0066-0. The cells were stained with an antibody recognizing the phosphorylated MELT motifs at Thr 943 and Thr 1155 of KNL1 (MELP^{T943/1155}) (Figure 3A). The phospho-KNL1 antibody specifically stained the kinetochores in control cells [32]. Upon treatment with NTRC 0066-0, the normalized kinetochore signal intensity of pKNL1 showed a reduction of more than 80% (Figure 3A).

Defects in SAC activity can lead to chromosome missegregations by allowing mitotic exit in the presence of misattached kinetochores. To address the effect of NTRC 0066-0 on the fidelity of chromosome segregation, we followed dividing HeLa cells stably expressing yellow fluorescent protein (YFP)-tagged histone H2B by time-lapse imaging (Figure 3B). Treatment with 30 nM NTRC 0066-0 decreased the time cells spent in mitosis from 1 h to ~30 min, while 100 nM NTRC 0066-0 reduced it to ~10 min (Figure 3C), a known effect of spindle checkpoint inhibition after TTK inactivation [38, 39]. Whereas 30 nM NTRC 0066-0 reduces time in mitosis, it was not sufficient to induce chromosome segregation errors (Figure 3D). In contrast, treatment with 100 nM NTRC 0066-0 led to a massive increase in chromosome missegregations (Figure 3D).

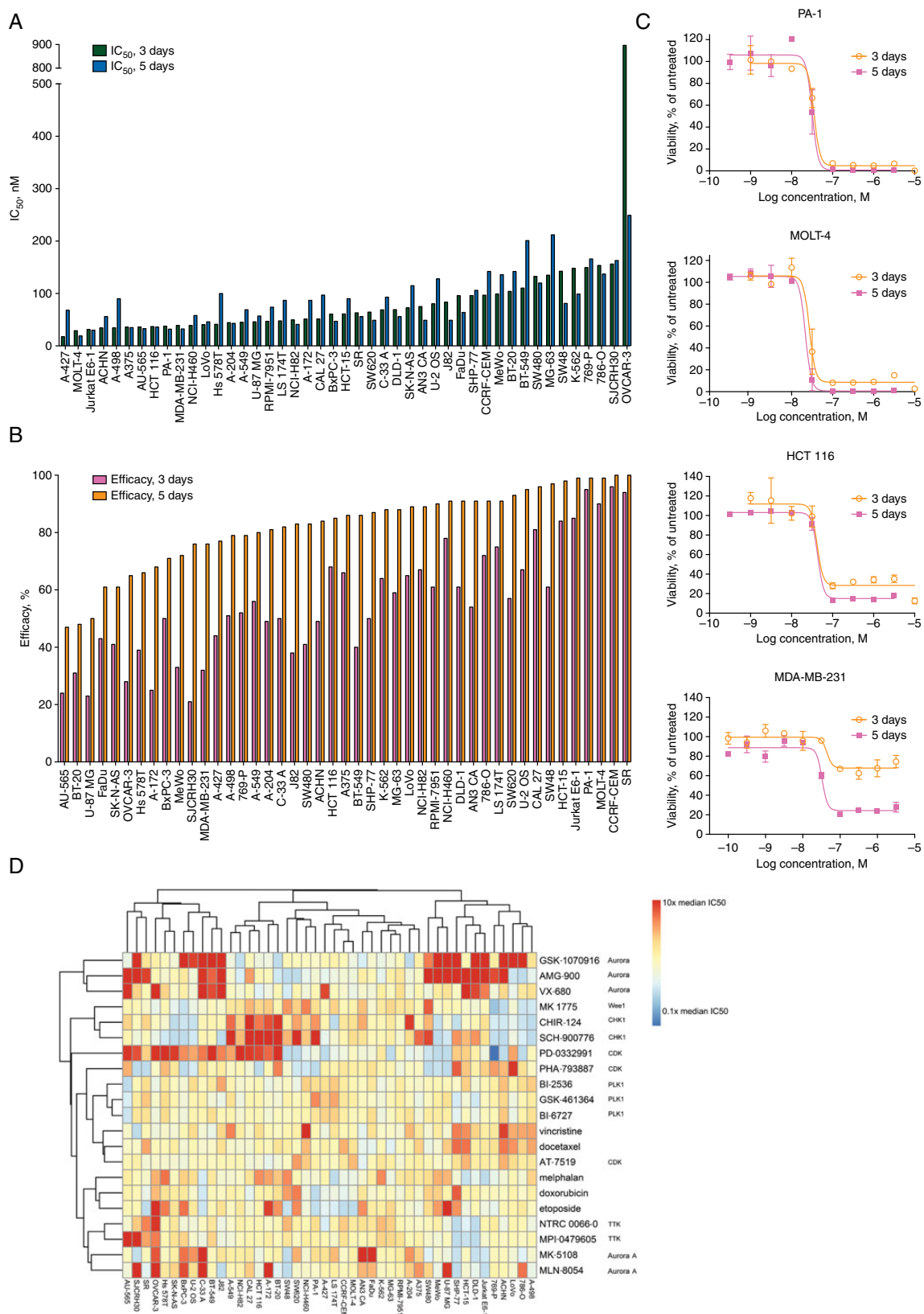


Figure 2. NTRC 0066-0 treatment inhibits cell proliferation. (A) IC₅₀ of NTRC 0066-0 in proliferation assays of 3 or 5 days on 45 cancer cell lines. Cell lines were ranked on IC₅₀ value in 3 days proliferation assay. (B) Maximum inhibitory effect (efficacy) in same proliferation assays as in (A). Cell lines were ranked on maximum inhibitory effect in 5 days proliferation assay. (C) Dose–response curves of NTRC 0066-0 in proliferation assays of 3 and 5 days with HCT-116, PA-1, MDA-MB-231 and MOLT-4 cells. (D) Hierarchical clustering of profiling data of TTK inhibitors, cytotoxic agents, PLK1 and Aurora kinase inhibitors in proliferation assays of 3 days on the 44 Oncolines™ cancer cell line panel. ¹⁰logIC₅₀s were used after median polishing.

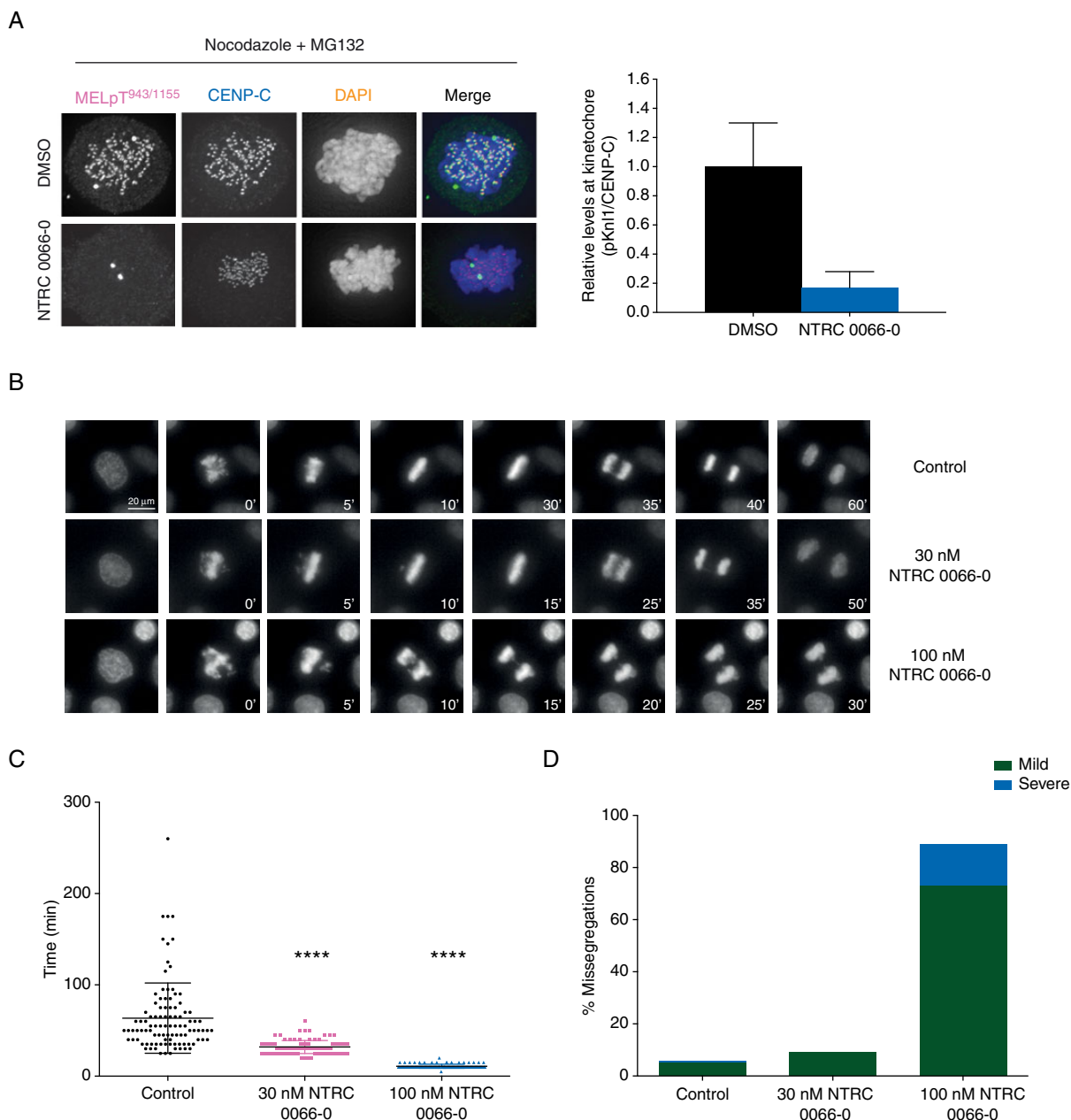


Figure 3. NTRC 0066-0 treatment leads to chromosome segregation errors in cell lines. (A) Representative images of HeLa cells stained with phospho-KNL1-specific antibody (MELpT^{943/1155}, gray (pink online)). Cells were treated with nocodazole/MG132 and 200 nM NTRC 0066-0 or vehicle (DMSO). Chromatin was visualized by staining with DAPI (light gray (orange online)) and kinetochores by staining with CENP-C antibodies (dark gray (blue online)). The graph depicts the normalized signal intensity (MELpT/CENP-C) of phospho-KNL1 staining at kinetochores in control and NTRC 0066-0-treated cells. (B) Representative examples of time-lapse imaging of HeLa cells expressing H2B-YFP in the absence or presence of NTRC 0066-0 (30 and 100 nM). Numbers show the time in minutes from the first frame in mitosis (time 0') till five frames after anaphase onset. (C) Scatter dot plot representation of the mean and standard deviation of time in mitosis (from nuclear envelope breakdown to anaphase onset) of control and NTRC 0066-0 treated HeLa cells ($n = 100$ per condition). Means are statistically different (asterisks), $P < 0.05$ (Dunn's test). Time spent in mitosis was 63.6 ± 38.5 min (mean \pm SD) for untreated cells (control), 32.0 ± 7.2 min for cells treated with 30 nM NTRC 0066-0 and 10.9 ± 2.2 min for cells treated with 100 nM NTRC 0066-0. (D) Quantification of mild and severe chromosome missegregations in HeLa cells expressing H2B-YFP, treated with 30 or 100 nM NTRC 0066-0 or vehicle ($n = 100$ cells per condition).

These results are in accordance with knockdown and inhibition of TTK with other inhibitors [34, 40, 41], although the NTRC 0066-0 concentrations used to obtain these effects were significantly lower, owing to the potency of the compound. This indicates that NTRC 0066-0 inhibits TTK in human cancer cells and modulates the physiological role of the kinase.

toxicity studies of NTRC 0066-0

Before investigating the efficacy of NTRC 0066-0 in tumor mouse models, we determined the metabolic stability, bioavailability and possible toxicity of the compound. To study the effect of NTRC 0066-0 on normal, nontransformed cells, we carried out proliferation assays with immortalized human

foreskin fibroblasts and retinal pigment epithelial cells. The IC_{50} of NTRC 0066-0 in these nontransformed cell lines was about two times higher than the average of cancer cell lines (supplementary Figure S1, available at *Annals of Oncology* online), indicating that this compound might be more selective in killing cancer cells.

In vitro metabolism assays showed that NTRC 0066-0 has good metabolic stability in liver microsomes, no interference with P-glycoprotein and negligible inhibition of hERG channel activity in patch clamp (supplementary Table S4, available at *Annals of Oncology* online). Bioavailability *in vivo* was determined after a single injection of NTRC 0066-0 i.p. or oral (p.o.) administration (supplementary Figure S2, available at *Annals of Oncology* online). NTRC 0066-0 showed good oral bioavailability ($F = 45\%$) and exposure levels (supplementary Table S5, available at *Annals of Oncology* online). Maximum exposure level (c_{max}) was even three times higher after i.p. administration (supplementary Table S5, available at *Annals of Oncology* online).

To determine the maximum tolerated treatment dose (MTTD) of NTRC 0066-0 and characterize possible toxic effects of the compound, we carried out a dose escalation study in female FVB wild-type mice (supplementary Figure S3, available at *Annals of Oncology* online). We observed that mice treated with 15 mg NTRC 0066-0 per kg body weight (15 mg/kg) were healthy and did not suffer weight loss. In contrast, a dose of 25 mg/kg NTRC 0066-0 resulted in severe weight loss 10 days after treatment.

To further characterize the *in vivo* activity of NTRC 0066-0, the highly proliferating tissues of treated mice were subjected to a pathological examination. Treatment with 25 mg/kg mainly affected the gut, where an increased number of apoptotic cells and a reduction in the number of intestinal crypts were observed (supplementary Table S6, available at *Annals of Oncology* online). Based on these analyses we concluded that within 15 mg/kg, NTRC 0066-0 shows limited gastrointestinal toxicity and no signs of other toxicity, such as hematological. Based on these observations, the MTTD of NTRC 0066-0 was set at 15 mg/kg, when dosed daily.

Because taxanes are a first-line standard of care treatment in TNBC, we investigated the effect of combining NTRC 0066-0 with docetaxel in a MTTD study. We observed weight loss in all groups treated with the combination of NTRC 0066-0 and docetaxel (supplementary Figure S3B, available at *Annals of Oncology* online). Histopathological analysis showed that docetaxel alone not only caused gastrointestinal toxicity, but also hematological toxicity (supplementary Table S6, available at *Annals of Oncology* online). Because NTRC 0066-0 could potentially exacerbate the toxicity of docetaxel, we decided to reduce the interval of treatments with NTRC 0066-0 to every other day in the following *in vivo* studies.

intervention studies in mouse models for human TNBC

To investigate whether NTRC 0066-0 could be a therapeutic approach in TNBC, we tested the inhibitor in tumors arising from xenografted MDA-MB-231 cells in BALB/C nude mice. About 20 mg/kg NTRC 0066-0 given orally every other day reduced tumor growth in this model by 61%, which is almost as efficient

as paclitaxel, given weekly at 15 mg/kg by i.v. injection (70%) (Figure 4A). In order to determine the effect of TTK inhibition alone, or in combination with taxanes, we used a murine breast cancer model that mimics human TNBC. The tumors originate from a $BRCA1^{-/-};TP53^{-/-}$ conditional knockout mouse strain, in which the expression of the $BRCA1$ and $TP53$ genes is inactivated through homologous recombination by the Cre recombinase, whose expression is under the keratin 14 promoter. This way, $BRCA1$ and $TP53$ inactivation are restricted to several epithelial tissues, including mammary and skin epithelia [42]. These mice spontaneously develop ER-negative mammary carcinomas that resemble human-basal-like breast cancer and present genomic instability [42]. To overcome the long latency of the tumors, a transplantation protocol was used in which pieces of the same $BRCA1^{-/-};TP53^{-/-}$ breast tumor donor were transplanted in different FVB strain wild-type mice. Additionally, this protocol ensures that all mice receive a tumor with the same genetic background. Tumor donors were included from MDR-proficient and MDR-deficient mice, which had been generated by inactivation of the mouse MDR P-glycoprotein genes $MDR1a$ and $MDR1b$ [43]. Treatments were initiated once the tumor reached a volume of $\geq 200 \text{ mm}^3$. Docetaxel treatment was interrupted when the tumor had regressed to below 50% of the initial size, while NTRC 0066-0 was maintained for 28 days (Figure 4B). Only when the tumor regrew and reached a volume of 200 mm^3 , docetaxel and/or NTRC 0066-0 treatments were re-initiated (Figure 4C).

The single treatment with 10 or 15 mg/kg NTRC 0066-0 showed no benefit in overall survival (Figure 4D). The median survival of mice treated with vehicle, 10 or 15 mg/kg NTRC 0066-0 was, respectively, 11, 12 and 12.5 days (supplementary Table S7, available at *Annals of Oncology* online).

It was previously reported that these $BRCA1^{-/-};TP53^{-/-}$ tumors initially respond to docetaxel treatment, but the tumors invariably acquire resistance to the taxane [31]. Consistently, we observed an increase in the median survival of mice treated with 25 mg/kg docetaxel in combination with vehicle (60 days) when compared with vehicle alone (11 days) (Figure 4E). Similar responses occurred in the MDR-proficient as well as in the MDR-deficient donors (data not shown). Duration of the response was, however, twice as long in the MDR-deficient mice, consistent with a role of P-glycoprotein in intrinsic docetaxel resistance in the tumors. Importantly, the beneficial treatment with docetaxel was enhanced by combining with 10 mg/kg NTRC 0066-0, which doubled the median survival from 60 to 121 days (Figure 4E). We observed that mice treated with TTK inhibitors underwent more cycles of tumor regression (supplementary Figure S4A, available at *Annals of Oncology* online). Strikingly, one of the mice from the group 25 mg/kg docetaxel + 10 mg/kg NTRC 0066-0 was in remission for 156 days. By the time the experiment was concluded, the histological analysis of the transplanted mammary fat pad showed that there were no tumor cells present (supplementary Figure S5, available at *Annals of Oncology* online).

The previous results suggest that the combination of docetaxel and TTK inhibition potentiates the cytotoxic effect of docetaxel. In order to maximize the effect of the combination therapy and, at the same time, reduce toxicity, we treated mice with 12.5 mg/kg docetaxel together with vehicle or 15 mg/kg NTRC 0066-0. In these conditions, the median survival increased from 50 to 90

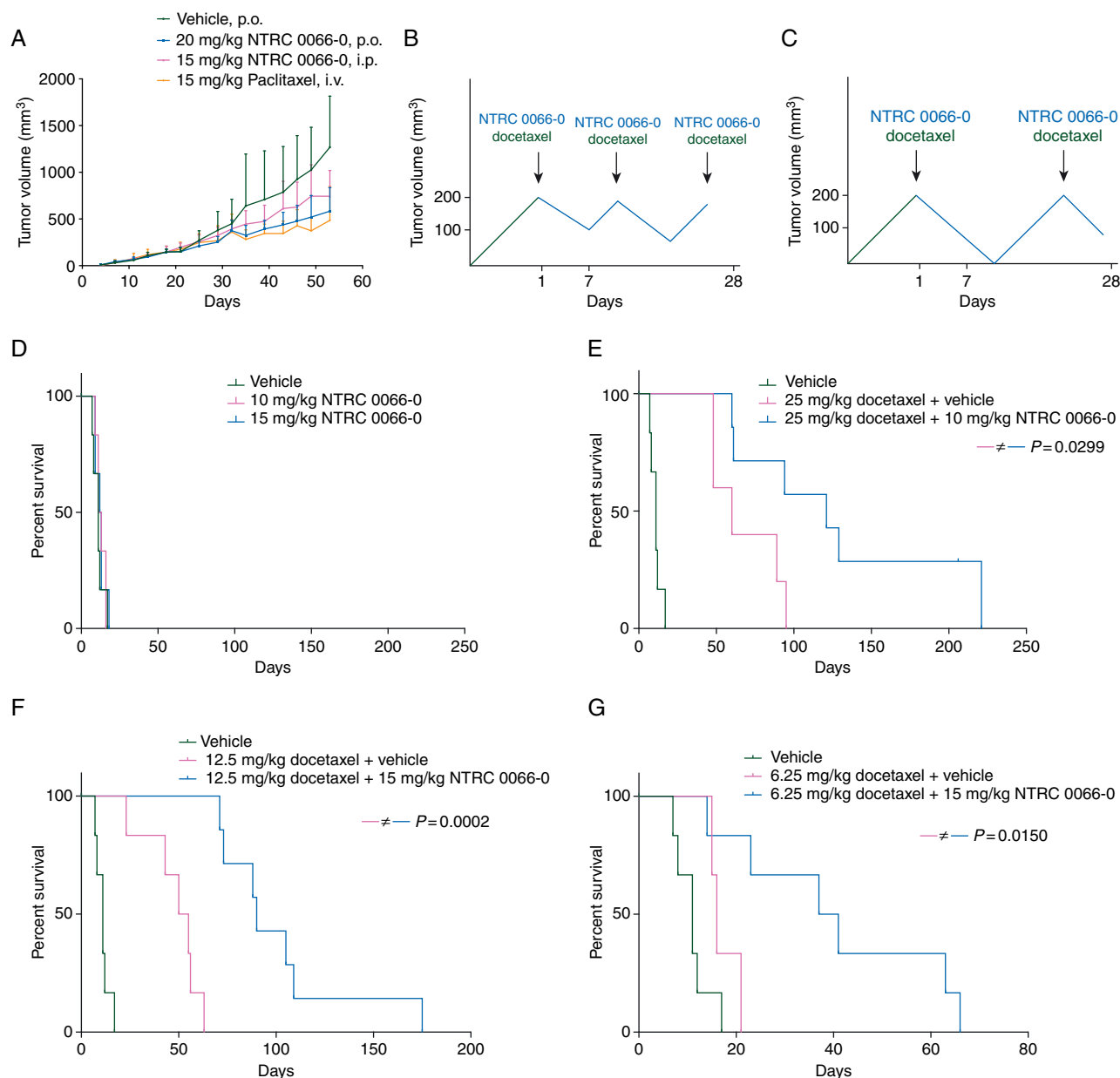


Figure 4. TTK inhibitors increase the efficacy of triple-negative breast cancer treatment. (A) Tumor growth curves (mean and standard error of the mean) of the orthotopic xenograft model of the TNBC cell line MDA-MB-231. Once the tumors reached a volume of 200 mm³, mice were treated with 20 mg/kg NTRC 0066-0, p.o., 15 mg/kg NTRC 0066-0, i.p., every other day, 15 mg/kg paclitaxel, i.v., once a week, or with vehicle ($n = 5$ mice per treatment group). (B and C) Dosing scheme and combinations of treatments in mice transplanted with BRCA1^{-/-};TP53^{-/-} mammary tumors. Arrows represent docetaxel treatments; solid gray (blue online) lines correspond to NTRC 0066-0 treatment. (D) Survival curves of mice treated with vehicle, 10 or 15 mg/kg NTRC 0066-0 ($n = 6$ for each group). (E) Survival curves of mice treated with 25 mg/kg docetaxel in combination with vehicle ($n = 5$) or 10 mg/kg NTRC 0066-0 ($n = 7$). (F) Survival curves of mice treated with 12.5 mg/kg docetaxel combined with vehicle ($n = 6$) or 15 mg/kg NTRC 0066-0 ($n = 7$). (G) Survival curves of mice treated with 6.25 mg/kg docetaxel in combination with vehicle and 15 mg/kg NTRC 0066-0 ($n = 6$ for each group). The log-rank P values are indicated.

days (Figure 4F), followed by a delay in tumor recurrence in the groups treated with NTRC 0066-0 (supplementary Figure S4B, available at *Annals of Oncology* online). To investigate the limits of docetaxel reduction, we treated mice with a subeffective dose of taxane (6.25 mg/kg). The combination of docetaxel and vehicle resulted in a median survival of 16 days, without tumor regression (supplementary Figure S4C, available at *Annals of Oncology* online). Strikingly, the combination of 6.25 mg/kg docetaxel with 15 mg/kg NTRC 0066-0 increased survival to 41 days

(Figure 4G), accompanied by tumor regression (supplementary Figure S4C, available at *Annals of Oncology* online). These data show that low-dose docetaxel in combination with NTRC 0066-0 results in the same therapeutic effect as obtained with docetaxel alone at a two times higher dose.

To address possible side-effects caused by the combination therapy, histopathological analysis of the tumors and highly proliferative tissues were carried out. Overall, no dramatic pathological changes in the intestine, spleen or bone marrow

were observed (supplementary Table S7, available at *Annals of Oncology* online). However, in-depth analysis of the tumors revealed some particular changes in cellular morphology in the groups treated with docetaxel, namely cellular pleomorphism (i.e. cells with multiple nuclei) and squamous cell metaplasia (supplementary Table S7, available at *Annals of Oncology* online). More importantly, prolonged treatment of mice with NTRC 0066-0 within the MTTD did not result in weight loss, or pathological changes in the gut, spleen or bone marrow, suggesting that TTK inhibition primarily affects CIN cells *in vivo*.

in vivo target engagement of NTRC 0066-0

The *in vivo* target engagement of NTRC 0066-0 was determined by scoring anaphase figures in the intestine and tumors from the different treatment groups (Figure 5A). Five appearances of anaphase figures were quantified: (i) normal; (ii) in the presence of lagging chromosomes; (iii) chromatin bridges or (iv) combination of both and (v) multipolar (Figure 5B). Since *BRCA1*^{-/-}; *TP53*^{-/-} tumors are chromosome unstable [42], the baseline of chromosome missegregations is higher in tumor samples in comparison to the gut (24% versus 6%, respectively). Single

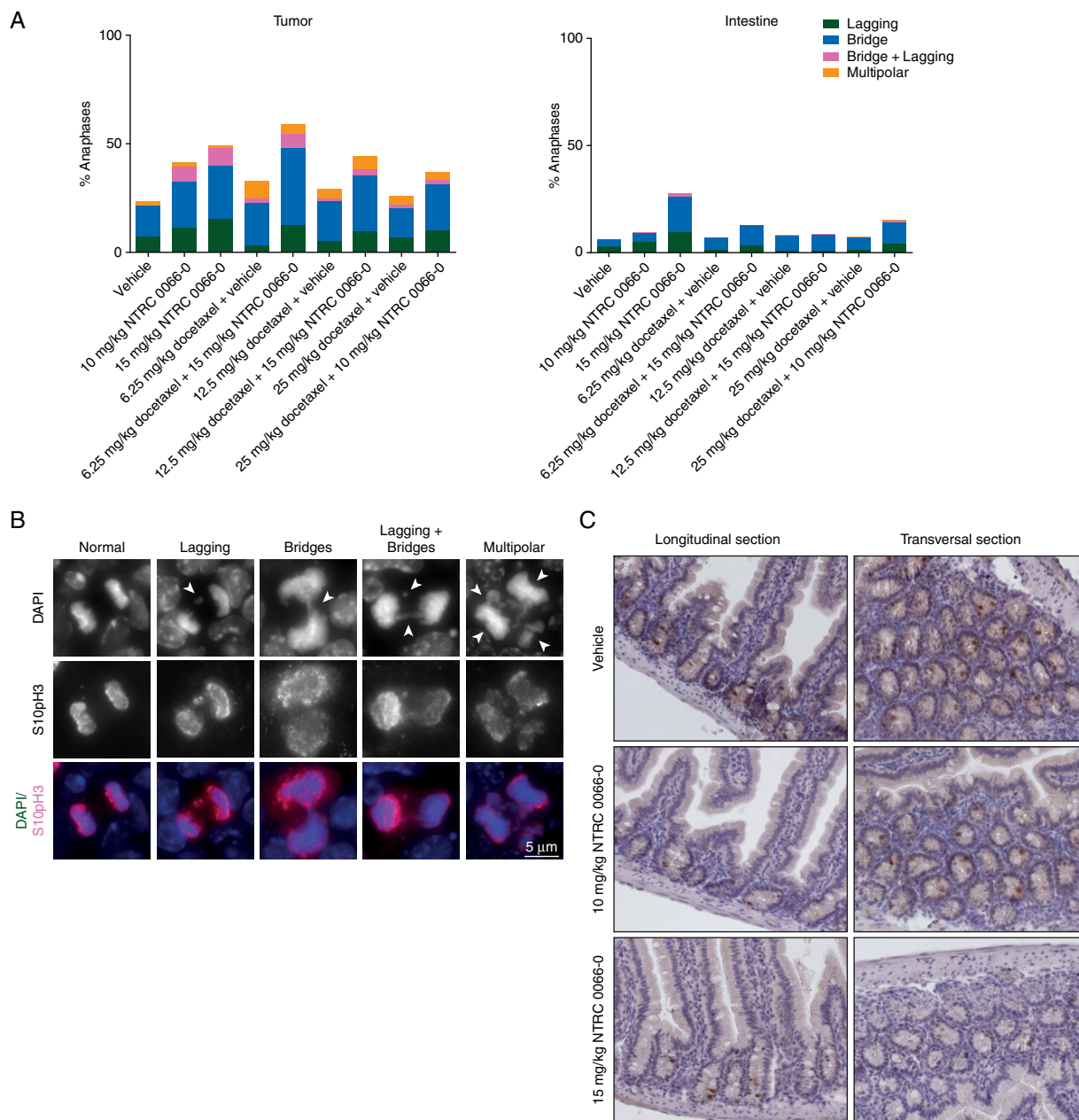


Figure 5. *In vivo* TTK inhibition increases the number of chromosome missegregations. (A) Quantification of abnormal anaphase figures in small intestine and breast tumors in mice treated with the indicated drugs. For each treatment condition, tissue sections from two different samples were immunostained for histone H3 phosphorylated on serine 10, and DNA counterstained with DAPI (~400 anaphases were scored per treatment). (B) Representative images of the anaphases scored in (A). Arrowheads show the abnormalities scored in each class. (C) Immunohistochemistry staining with MELpT^{943/1155} antibody of longitudinal tissue sections (left) and transverse tissue sections (right) of the small intestine from mice treated with vehicle, 10 and 15 mg/kg NTRC 0066-0.

treatment with NTRC 0066-0 led to a dose-dependent increase in chromosome segregation errors both in the intestine and in tumor cells (Figure 5A), similar to what was observed in cultured cancer cells (Figure 3). In all samples treated with docetaxel and NTRC 0066-0, more chromosome missegregations were observed in comparison to vehicle-treated (Figure 5A). In addition, samples treated with docetaxel presented higher levels of spindle multipolarity. The highest percentage of erroneous anaphases occurred in tumors treated with 6.25 mg/kg docetaxel combined with 15 mg/kg NTRC 0066-0. We conclude that NTRC 0066-0 treatment impairs chromosome segregation *in vivo*, consistent with inhibition of TTK *in vivo*.

To further determine target engagement of the inhibitor, the intestine of mice treated with vehicle, or NTRC 0066-0 were stained with the KNL1-MELP^{T943/1155} antibody. The antibody strongly stains mitotic cells in the crypt and transit-amplifying compartment, but signal intensity in the mitotic cells was reduced upon treatment with inhibitor (Figure 5C). Therefore,

both the chromosome segregation errors and the reduction of KNL1-MELP^{T943/1155} phosphorylation signal provide evidence that the antitumor effects of NTRC 0066-0 result from its *in vivo* inhibition of TTK.

TTK inhibition increases the efficiency of docetaxel chemotherapy in mice

The effects of combination treatment can depend on whether individual components are administered sequentially or simultaneously [44]. For this reason, we carried out a second intervention study, in which we determined whether NTRC 0066-0 could work as a maintenance therapy after docetaxel treatment. Using the same tumor model and transplantation protocol, mice were treated with 12.5 mg/kg docetaxel in combination with vehicle or with 15 mg/kg NTRC 0066-0. In one cohort, docetaxel was combined with NTRC 0066-0 from the beginning of therapy (Figure 6A). In a second cohort, treatment with

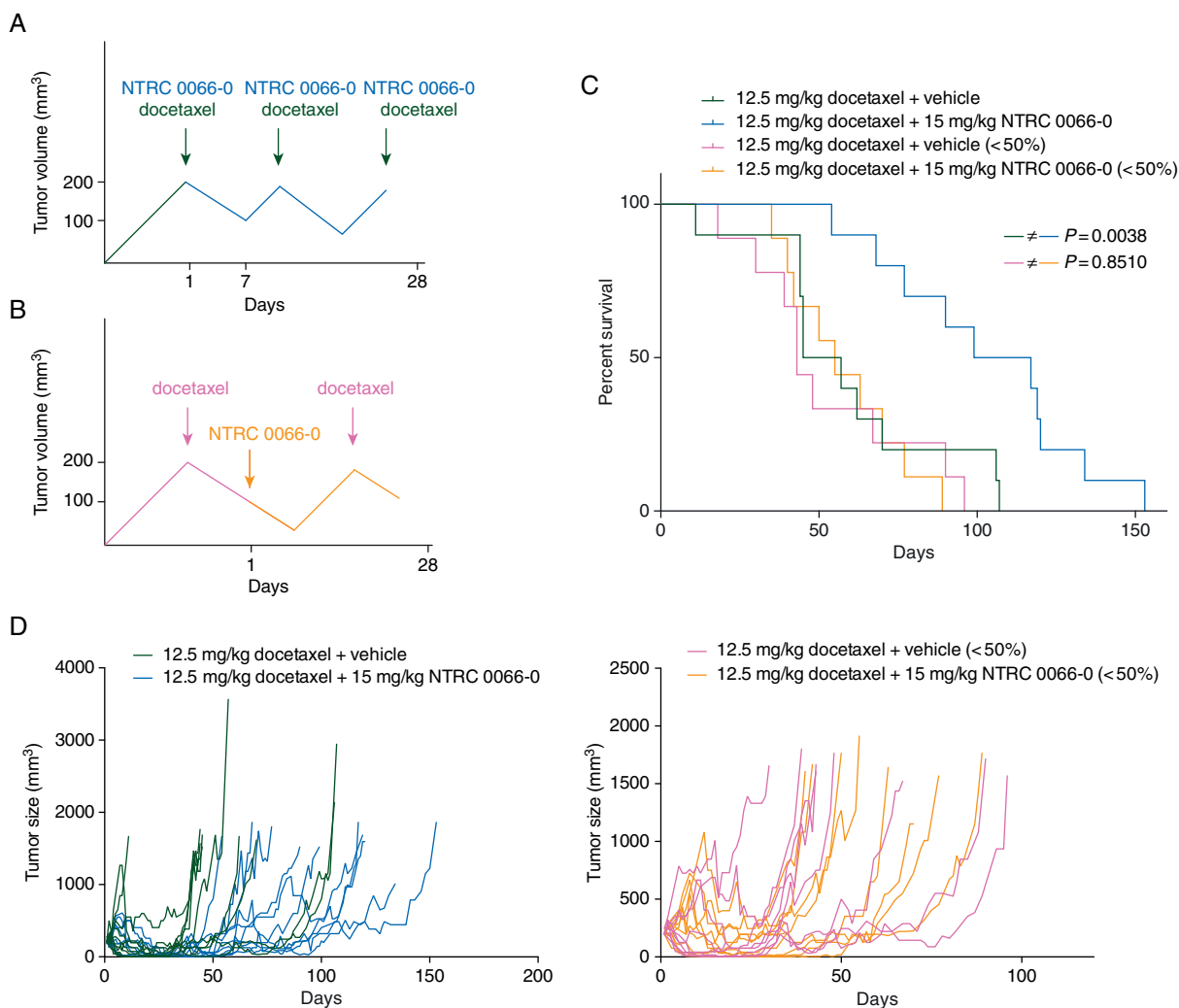


Figure 6. Maximum *in vivo* efficacy of NTRC 0066-0 and docetaxel occurs when the drugs are administered at the same time. (A and B) Schematic representation of dosing scheme and combinations. Dark gray (green online) arrows represent docetaxel treatments; arrows and continuous gray (blue online) or light gray (orange online) lines correspond to NTRC 0066-0 treatment. (C) Survival curves of mice treated with 12.5 mg/kg docetaxel combined with vehicle or 15 mg/kg NTRC 0066-0. The difference between the two treatment arms is that NTRC 0066-0 was given only once the tumor regressed to 50% of its initial size, and not from the beginning. The log-rank *P* values are indicated. (D) Growth curves of the BRCA1^{-/-};TP53^{-/-} breast tumors orthotopically transplanted and treated with the different combinations.

NTRC 0066-0 was only started once the tumor had regressed to 50% of its initial size due to docetaxel treatment (Figure 6B).

In accordance to the previous results (Figure 4), co-treatment with NTRC 0066-0 and docetaxel doubled the survival of mice in comparison to docetaxel with vehicle treatment (Figure 6C). Median survival changed from 51 days in the vehicle-treated group to 108 days in the NTRC 0066-0 treated mice, and the tumors treated with NTRC 0066-0 clearly took longer to relapse (Figure 6D). However, mice treated with NTRC 0066-0 after tumor regression showed no benefit in survival (median survival was 43 days in the vehicle-treated group and 55 days in the NTRC 0066-0-treated mice, Figure 6C) or tumor regression (Figure 6D). These results indicate that NTRC 0066-0 and docetaxel are best combined simultaneously to potentiate the effect of docetaxel.

discussion

Targeted therapies bring great benefit to cancer patients, because they can improve survival rates with fewer side-effects than traditional, less cytotoxic drugs. Small molecule inhibitors of protein kinases are a prime example of the success of targeted therapy. Many of these inhibitors exploit unique features of tumor cells, permitting cancer specificity while having limited effects on healthy cells. Here, we have taken advantage of TTK overexpression in TNBC [4–6] and developed a selective inhibitor of TTK. NTRC 0066-0 inhibits TTK enzyme activity with subnanomolar potency and is more than 200 times selective over all other kinases tested, resulting in a selectivity entropy [30] (S_{sel}) of 0.26, ranking NTRC 0066-0 among the 8% most selective kinase inhibitors for which broad kinome profiling data have been published [30, 45]. In comparison to other published TTK inhibitors, NTRC 0066-0 stands out with respect to its cellular activity, which may be related to its long residence on the target, as revealed in surface plasmon resonance experiments.

Knockdown experiments with short hairpin RNAs against TTK have suggested that nontransformed cells are less sensitive to TTK inhibition than cancer cell lines [5, 34]. In line with this, the IC_{50} of nontransformed cells was about two times higher than the average IC_{50} of a large panel of cancer cell lines examined. Importantly, prolonged treatment of mice with NTRC 0066-0 within the MTTD did not result in weight loss, or pathological changes in the gut, spleen or bone marrow. The MTTD of NTRC 0066-0 was determined by gastrointestinal toxicity, as evidenced by weight loss and an increased number of apoptotic cells in the intestinal crypts. The percentage of chromosome missegregations in intestinal tissue after TTK inhibition also remains well below the level in tumor tissue (Figure 5A), suggesting that TTK inhibition primarily affects CIN cells *in vivo*. We conclude that, within the MTTD, TTK inhibition by NTRC 0066-0 does not compromise the function of normal tissues.

NTRC 0066-0 resulted in inhibition of tumor growth in a xenograft of the TNBC cell line MDA-MB-231, but no efficacy was seen with NTRC 0066-0 monotherapy in a genetic mouse model that was used to explore the potential synergy of NTRC 0066-0 with taxane therapy. In this model, tumors regressed when NTRC 0066-0 was combined with a low dose of docetaxel. The reason for the lack of efficacy of NTRC 0066-0 monotherapy in this model is unclear. We hypothesize that this may be

because the number of chromosome segregation errors in the tumors is below the threshold that results in sufficient cell death to cause tumor regression. In future experiments, it will be interesting to increase the NTRC 0066-0 dose while decreasing the number of treatments. We expect that the long residence time of the inhibitor in the kinase might compensate for the reduction in the number of treatments and increase the cytotoxic effect in the tumors without comprising normal cell viability.

Simultaneous administration of docetaxel and NTRC 0066-0 greatly increased the survival of mice with TNBC. This response is most likely due to increased chromosome segregation errors, because in all samples treated with docetaxel and NTRC 0066-0 an increased number of missegregations was observed in comparison to vehicle-treated (Figure 5A). In comparison to NTRC 0066-0 monotherapy, we did not observe an increased number of missegregations upon combination treatment. However, this discrepancy could be entirely due to the fact that the tumors are harvested at the time they were no longer sensitive to docetaxel treatment. In terms of segregation errors, the strongest effect of NTRC 0066-0 was achieved at the lowest dose of docetaxel (i.e. 6.25 mg/kg). It may be that these tumors did not have time to acquire taxane resistance. This way, by the time the tumors were collected, the maximum docetaxel effect was observed. The analysis of tumor samples right after docetaxel and NTRC 0066-0 treatment could help to clarify whether the increased number of chromosome segregation errors drives the enhanced cytotoxicity.

The mechanism underlying the activity of low dose of docetaxel and NTRC 0066-0 is complex. Despite the clinical use of taxanes for more than two decades, their mechanism of action *in vivo* is still not understood. Whereas in tissue culture taxanes hyperstabilize spindle microtubules and induce mitotic arrest, intravital imaging of murine xenografts did not show any evidence of mitotic arrest resulting from taxol treatment [46, 47]. A recent study has shown that paclitaxel treatment in breast cancer patients results in more multipolar spindles and chromosome missegregations that are not necessarily followed by mitotic arrest [48]. Consistent with these observations, we found that docetaxel increases the number of multipolar spindles and the combination with NTRC 0066-0 did not affect multipolarity (Figure 5A). In addition, the tumors treated with docetaxel presented pleomorphism and multinucleation (supplementary Table S7, available at *Annals of Oncology* online), a readout of chromosome instability. We therefore propose that treatment with docetaxel increases the number of multipolar spindles, and that the combination with NTRC 0066-0 drives these multipolar spindles out of mitosis, causing massive chromosome segregation errors leading to more tumor cell death. We propose NTRC 0066-0 as a novel neoadjuvant therapy in the treatment of TNBC. Further preclinical toxicological profiling has been initiated to prepare for proof-of-concept clinical studies in TNBC patients.

acknowledgements

We thank the personnel of the Netherlands Cancer Institute animal facilities for excellent animal care; the departments of Pathology and Animal Pathology for assistance in immunohistochemical stainings; Sven Rottenberg for providing the MDR-

deficient tumor donors; Olaf van Tellingen for pharmacokinetic studies. We also thank Joeri de Wit at Netherlands Translational Research Center B.V. for synthesis of reference inhibitors.

funding

This research was supported by grants from Top Institute Pharma (T3-503), the Innovation Office of the Ministry of Economic Affairs of the Netherlands (INT 111039), NWO-Vici (865.12.004), Marie Curie Initial Training Network (ITN-2013-607722 PloidyNet) and NWO Gravitation Program (Cancer Genomics Center, CGC.nl). The funders had no role in study design, data collection and analysis, decision to publish or preparation of the manuscript.

disclosure

GJRZ and RCB are founders and shareholders of Netherlands Translational Research Center B.V. All remaining authors have declared no conflicts of interest.

references

- Sotiriou C, Pusztai L. Gene-expression signatures in breast cancer. *N Engl J Med* 2009; 360: 790–800.
- Foulkes WD, Smith IE, Reis-Filho JS. Triple-negative breast cancer. *N Engl J Med* 2010; 363: 1938–1948.
- A'Hern RP, Jamal-Hanjani M, Szasz AM et al. Taxane benefit in breast cancer—a role for grade and chromosomal stability. *Nat Rev Clin Oncol* 2013; 10: 357–364.
- Al-Ejeh F, Simpson PT, Sanus JM et al. Meta-analysis of the global gene expression profile of triple-negative breast cancer identifies genes for the prognostication and treatment of aggressive breast cancer. *Oncogenesis* 2014; 3: e100.
- Daniel J, Coulter J, Woo JH et al. High levels of the Mps1 checkpoint protein are protective of aneuploidy in breast cancer cells. *Proc Natl Acad Sci USA* 2011; 108: 5384–5389.
- Maire V, Baldeyron C, Richardson M et al. TTK/hMPS1 is an attractive therapeutic target for triple-negative breast cancer. *PLoS One* 2013; 8: e63712.
- Liu X, Winey M. The MPS1 family of protein kinases. *Ann Rev Biochem* 2012; 81: 561–585.
- Sacristan C, Kops GJ. Joined at the hip: kinetochores, microtubules, and spindle assembly checkpoint signaling. *Trends Cell Biol* 2015; 25: 21–28.
- Baker DJ, Chen J, van Deursen JM. The mitotic checkpoint in cancer and aging: what have mice taught us? *Curr Opin Cell Biol* 2005; 17: 583–589.
- Kops GJ, Foltz DR, Cleveland DW. Lethality to human cancer cells through massive chromosome loss by inhibition of the mitotic checkpoint. *Proc Natl Acad Sci USA* 2004; 101: 8699–8704.
- Michel L, Diaz-Rodriguez E, Narayan G et al. Complete loss of the tumor suppressor MAD2 causes premature cyclin B degradation and mitotic failure in human somatic cells. *Proc Natl Acad Sci USA* 2004; 101: 4459–4464.
- Kilpinen S, Ojala K, Kallioniemi O. Analysis of kinase gene expression patterns across 5681 human tissue samples reveals functional genomic taxonomy of the kinome. *PLoS One* 2010; 5: e15068.
- Landi MT, Dracheva T, Rotunno M et al. Gene expression signature of cigarette smoking and its role in lung adenocarcinoma development and survival. *PLoS One* 2008; 3: e1651.
- Liang XD, Dai YC, Li ZY et al. Expression and function analysis of mitotic checkpoint genes identifies TTK as a potential therapeutic target for human hepatocellular carcinoma. *PLoS One* 2014; 9: e97739.
- Mills GB, Schmandt R, McGill M et al. Expression of TTK, a novel human protein kinase, is associated with cell proliferation. *J Biol Chem* 1992; 267: 16000–16006.
- Salvatore G, Nappi TC, Salerno P et al. A cell proliferation and chromosomal instability signature in anaplastic thyroid carcinoma. *Cancer Res* 2007; 67: 10148–10158.
- Slee RB, Grimes BR, Bansal R et al. Selective inhibition of pancreatic ductal adenocarcinoma cell growth by the mitotic MPS1 kinase inhibitor NMS-P715. *Mol Cancer Ther* 2014; 13: 307–315.
- Tannous BA, Kerami M, Van der Stoop PM et al. Effects of the selective MPS1 inhibitor MPS1-IN-3 on glioblastoma sensitivity to antimetabolic drugs. *J Natl Cancer Inst* 2013; 105: 1322–1331.
- Yuan B, Xu Y, Woo JH et al. Increased expression of mitotic checkpoint genes in breast cancer cells with chromosomal instability. *Clin Cancer Res* 2006; 12: 405–410.
- Lengauer C, Kinzler KW, Vogelstein B. Genetic instability in colorectal cancers. *Nature* 1997; 386: 623–627.
- Carter SL, Eklund AC, Kohane IS et al. A signature of chromosomal instability inferred from gene expression profiles predicts clinical outcome in multiple human cancers. *Nat Genet* 2006; 38: 1043–1048.
- Sheffer M, Bacolod MD, Zuk O et al. Association of survival and disease progression with chromosomal instability: a genomic exploration of colorectal cancer. *Proc Natl Acad Sci USA* 2009; 106: 7131–7136.
- Walther A, Houlston R, Tomlinson I. Association between chromosomal instability and prognosis in colorectal cancer: a meta-analysis. *Gut* 2008; 57: 941–950.
- Colombo R, Caldarelli M, Mennecozzi M et al. Targeting the mitotic checkpoint for cancer therapy with NMS-P715, an inhibitor of MPS1 kinase. *Cancer Res* 2010; 70: 10255–10264.
- Jemaa M, Galluzzi L, Kepp O et al. Characterization of novel MPS1 inhibitors with preclinical anticancer activity. *Cell Death Differ* 2013; 20: 1532–1545.
- Lauffer R, Ng G, Liu Y et al. Discovery of inhibitors of the mitotic kinase TTK based on N-(3-(3-sulfamoylphenyl)-1H-indazol-5-yl)-acetamides and carboxamides. *Bioorg Med Chem* 2014; 22: 4968–4997.
- Tardif KD, Rogers A, Cassiano J et al. Characterization of the cellular and antitumor effects of MPI-0479605, a small-molecule inhibitor of the mitotic kinase Mps1. *Mol Cancer Ther* 2011; 10: 2267–2275.
- Argyriou AA, Koltzenburg M, Polychronopoulos P et al. Peripheral nerve damage associated with administration of taxanes in patients with cancer. *Crit Rev Oncol Hematol* 2008; 66: 218–228.
- Hilkens PH, Verweij J, Vecht CJ et al. Clinical characteristics of severe peripheral neuropathy induced by docetaxel (Taxotere). *Ann Oncol* 1997; 8: 187–190.
- Uitdehaag JC, de Roos JA, van Doormalen AM et al. Comparison of the cancer gene targeting and biochemical selectivities of all targeted kinase inhibitors approved for clinical use. *PLoS One* 2014; 9: e92146.
- Rottenberg S, Nygren AO, Pajic M et al. Selective induction of chemotherapy resistance of mammary tumors in a conditional mouse model for hereditary breast cancer. *Proc Natl Acad Sci USA* 2007; 104: 12117–12122.
- Nijenhuis W, Vallardi G, Teixeira A et al. Negative feedback at kinetochores underlies a responsive spindle checkpoint signal. *Nat Cell Biol* 2014; 16: 1257–1264.
- Hewitt L, Tighe A, Santaguida S et al. Sustained Mps1 activity is required in mitosis to recruit O-Mad2 to the Mad1-C-Mad2 core complex. *J Cell Biol* 2010; 190: 25–34.
- Janssen A, Kops GJ, Medema RH. Elevating the frequency of chromosome mis-segregation as a strategy to kill tumor cells. *Proc Natl Acad Sci USA* 2009; 106: 19108–19113.
- Chou TC, Depew KM, Zheng YH et al. Reversal of anticancer multidrug resistance by the ardeemins. *Proc Natl Acad Sci USA* 1998; 95: 8369–8374.
- Masuda A, Maeno K, Nakagawa T et al. Association between mitotic spindle checkpoint impairment and susceptibility to the induction of apoptosis by anti-microtubule agents in human lung cancers. *Am J Pathol* 2003; 163: 1109–1116.
- Yamagishi Y, Yang CH, Tanno Y, Watanabe Y. MPS1/Mph1 phosphorylates the kinetochore protein KNL1/Spc7 to recruit SAC components. *Nat Cell Biol* 2012; 14: 746–752.
- Maciejowski J, George KA, Terret ME et al. Mps1 directs the assembly of Cdc20 inhibitory complexes during interphase and mitosis to control M phase timing and spindle checkpoint signaling. *J Cell Biol* 2010; 190: 89–100.

39. Sliedrecht T, Zhang C, Shokat KM, Kops GJ. Chemical genetic inhibition of Mps1 in stable human cell lines reveals novel aspects of Mps1 function in mitosis. *PLoS One* 2010; 5: e10251.
40. Kwiatkowski N, Jelluma N, Filippakopoulos P et al. Small-molecule kinase inhibitors provide insight into Mps1 cell cycle function. *Nat Chem Biol* 2010; 6: 359–368.
41. Santaguida S, Tighe A, D'Alise AM et al. Dissecting the role of MPS1 in chromosome biorientation and the spindle checkpoint through the small molecule inhibitor reversine. *J Cell Biol* 2010; 190: 73–87.
42. Liu X, Holstege H, van der Gulden H et al. Somatic loss of BRCA1 and p53 in mice induces mammary tumors with features of human BRCA1-mutated basal-like breast cancer. *Proc Natl Acad Sci USA* 2007; 104: 12111–12116.
43. Jaspers JE, Kersbergen A, Boon U et al. Loss of 53BP1 causes PARP inhibitor resistance in Brca1-mutated mouse mammary tumors. *Cancer Discov* 2013; 3: 68–81.
44. Solit DB, She Y, Lobo J et al. Pulsatile administration of the epidermal growth factor receptor inhibitor gefitinib is significantly more effective than continuous dosing for sensitizing tumors to paclitaxel. *Clin Cancer Res* 2005; 11: 1983–1989.
45. Davis MI, Hunt JP, Herrgard S et al. Comprehensive analysis of kinase inhibitor selectivity. *Nat Biotechnol* 2011; 29: 1046–1051.
46. Janssen A, Beerling E, Medema R, van Rheenen J. Intravital FRET imaging of tumor cell viability and mitosis during chemotherapy. *PLoS One* 2013; 8: e64029.
47. Orth JD, Kohler RH, Fojter F et al. Analysis of mitosis and antimitotic drug responses in tumors by in vivo microscopy and single-cell pharmacodynamics. *Cancer Res* 2011; 71: 4608–4616.
48. Zasadil LM, Andersen KA, Yeum D et al. Cytotoxicity of paclitaxel in breast cancer is due to chromosome missegregation on multipolar spindles. *Sci Transl Med* 2014; 6: 229–243.